

Supplementary Materials

1. Sputtered Depth for Low Index Cu Crystal Plane

Sputter yields of low index planes of Cu single crystal have been reported by Magnuson and Carlston [1]. Sputter yields of Cu (111), (100), and (110) by Ar ions with 1 kV are 4.1–4.5, ~3.4, and 1.9, respectively [1]. It is noted that the 1 kV for acceleration of Ar ions is the same condition to our experiment.

We calculated sputtered depth of Cu for each crystal planes. The sputtered depth d_{sp} can be described as:

$$S \times N_{Ar} = A_S \times D_a \times \frac{d_{sp}}{d_p}$$

where S is the sputter yield, N_{Ar} is number of Ar ions, A_S is area of sputtering, D_a is atomic density on the crystal plane, and d_p is distance of the lattice planes. Each value is summarized in Table S1. Therefore, d_{sp} of Cu (111), (100), and (110) are written as:

$$d_{sp}(111) = 1.0 \sim 1.1 \times \frac{a^3 N_{Ar}}{A_S}$$

$$d_{sp}(100) = 0.85 \times \frac{a^3 N_{Ar}}{A_S}$$

$$d_{sp}(110) = 0.95 \times \frac{a^3 N_{Ar}}{A_S}$$

where a is lattice constant of copper.

Table S1. Summary of d_p , D_a , S , and d_{sp} for Cu (111), (100), and (110).

Crystal Plane	d_p (m): Lattice Plane Distance	D_a (m ²): Atomic Density on The Plane	S (Atoms/Ion): Sputter Yield by 1 kV Ar Ion [1]	d_{sp} (m): Depth by Sputtering
(111)	$\frac{a}{4\sqrt{3}}$	$\frac{1}{\sqrt{3}a^2}$	4.1 ~ 4.5	$1.0 \sim 1.1 \times \frac{a^3 N_{Ar}}{A_S}$
(100)	$\frac{a}{2}$	$\frac{2}{a^2}$	3.4	$0.85 \times \frac{a^3 N_{Ar}}{A_S}$
(110)	$\frac{a}{\sqrt{2}}$	$\frac{\sqrt{2}}{a^2}$	1.9	$0.95 \times \frac{a^3 N_{Ar}}{A_S}$

Note: a is lattice constant of copper. N_{Ar} is number of argon ions. A_S is area sputtered by argon ions with 1 kV

2. Cu Domains

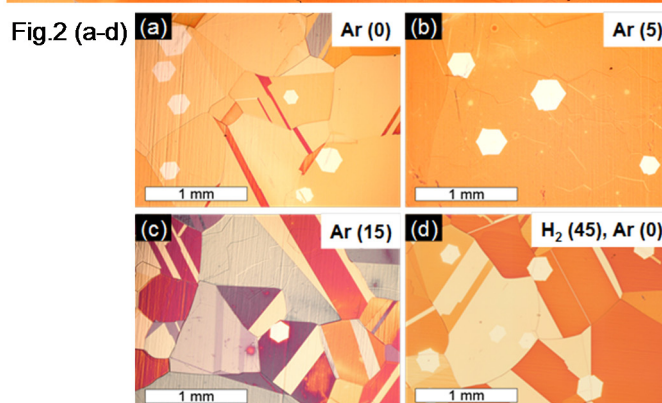
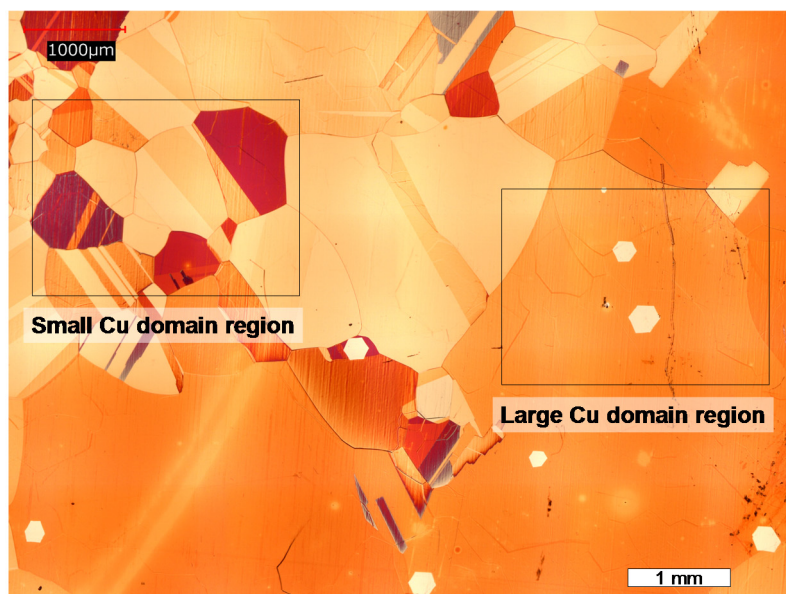


Figure S1. (Upper) Large area optical microscope image of CVD graphene on Cu with Ar annealing for 5 min, which is the same sample as Figure 2b. (Lower) Figure 2a–d. Scales of all images are adjusted to be same. Black rectangles in the upper image are same size as Figure 2a–d.

3. Spatial Uniformity of Graphene Nucleation

Table S2. The averages and the standard errors of the densities of graphene domains in Figure 2e.

		Ar Annealing Time (min)				
H ₂ /CH ₄		0	5	10	15	20
15/500		$72 \pm 2 \text{ cm}^{-2}$	$19 \pm 3 \text{ cm}^{-2}$	$5.5 \pm 0.4 \text{ cm}^{-2}$	$2.2 \pm 0.3 \text{ cm}^{-2}$	–
15/1000		–	–	$61 \pm 16 \text{ cm}^{-2}$	$17 \pm 7 \text{ cm}^{-2}$	$9 \pm 1 \text{ cm}^{-2}$

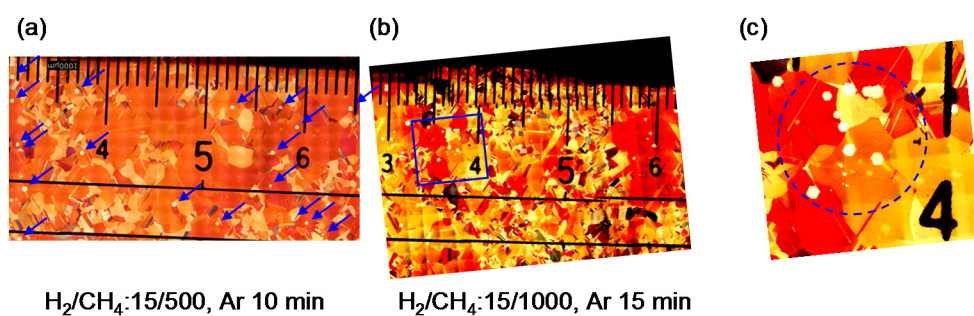


Figure S2. Large area optical microscope images of CVD graphene on Cu with (a) the H_2/CH_4 flow rate of 15/500 and the Ar annealing for 10 min, and (b) the H_2/CH_4 flow rate of 15/1000 and the Ar annealing for 15 min. Arrows in (a) indicate graphene domains; (c) Magnified image in (b).

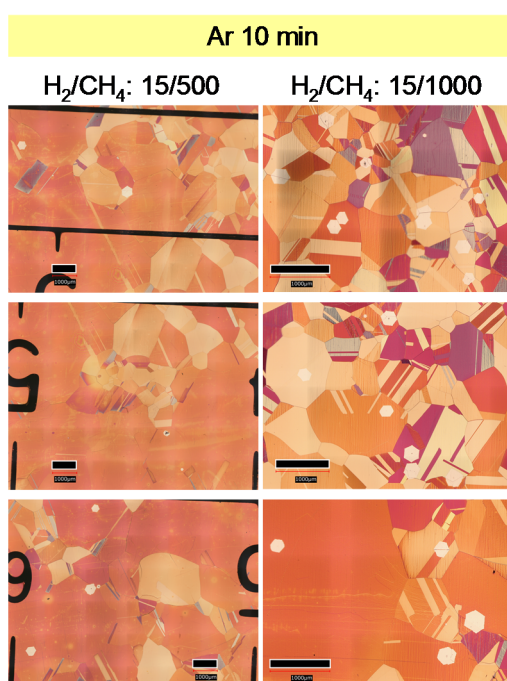


Figure S3. Optical microscope images of CVD graphene on Cu with the H_2/CH_4 flow rate of 15/500 and 15/1000, and the Ar annealing for 10 min. The variations of the density of graphene at different locations are compared.

4. LMM Auger by XPS

Figure S4 shows a high resolution Cu LMM auger spectrum of an Ar annealed Cu. The spectrum showed that Cu + CuO and Cu_2O peaks at 567.8 and 570.0 eV, respectively. The peak position of Cu_2O is consistent with a previous report [2]. The peak position of Cu + CuO is 0.2 eV lower than the previous report but higher than CuO (568.5 eV) in the table 1, indicating the existence of metallic Cu. Therefore, the result of Cu LMM is consistent with the discussion for Cu_2O in our manuscript.

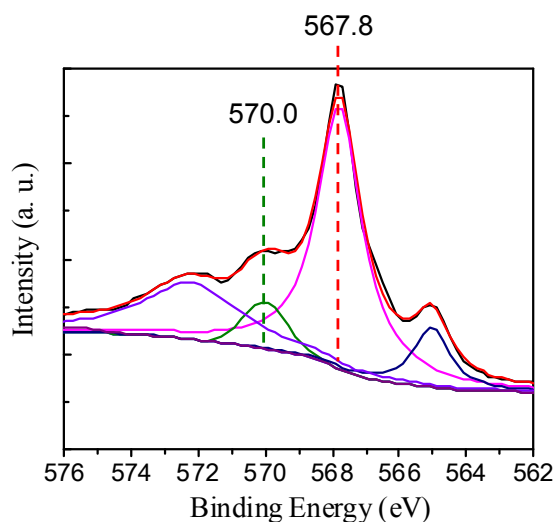


Figure S4. High resolution Cu LMM auger spectrum of an Ar annealed Cu. The spectrum is taken at the 2 nm deeper position than surface.

5. Concentration of residual oxygen in CVD chamber

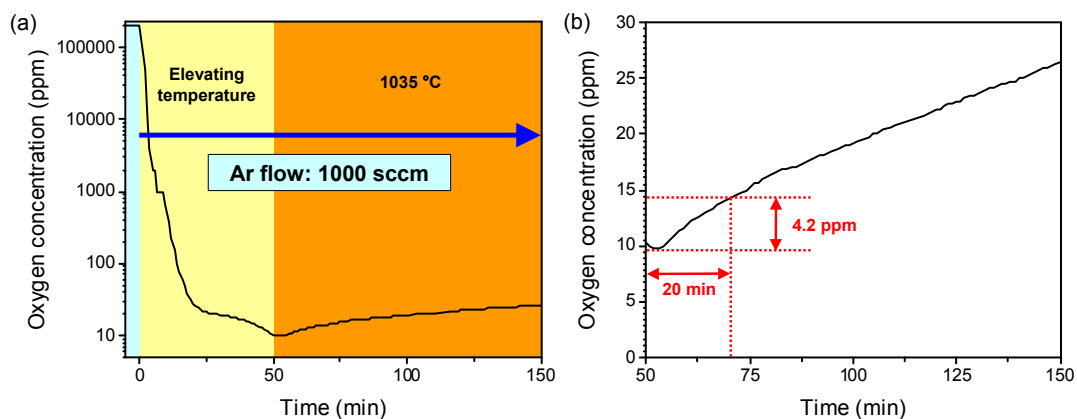


Figure S5. (a) Transition of residual oxygen in the CVD chamber. 1000 sccm Ar flowing was started at 0 min, and elevating temperature started at 1 min from room temperature. The temperature was reached at 1035 °C after 50 min. The chamber pressure was ~0.12 MPa; (b) Enlarged graph of (a) after 50 min.

6. Cu Oxide Can Be Formed by Segregation Process or Not?

To examine copper oxide forms during Ar annealing of cooling process, we did *in situ* heating in XPS chamber for the Cu foil after annealing in Ar for 65 min.

The Cu sample was prepared with H₂/Ar annealing for 15 min and Ar annealing for 65 min, and were then cooled down under Ar ambient without growth process. The sample after the CVD process was transferred to the XPS chamber within 11 min.

Figure S6 shows O1s spectra recorded at each temperature. The temperature was elevated from room temperature (RT) (top spectrum) to 800 °C and then naturally cooled down to RT (the lowest spectrum). The oxygen signal was completely disappeared at 800 °C. After cooling to RT, any oxygen signals were not observed indicating that Cu oxide is not formed by segregation during the cooling in the present CVD process.

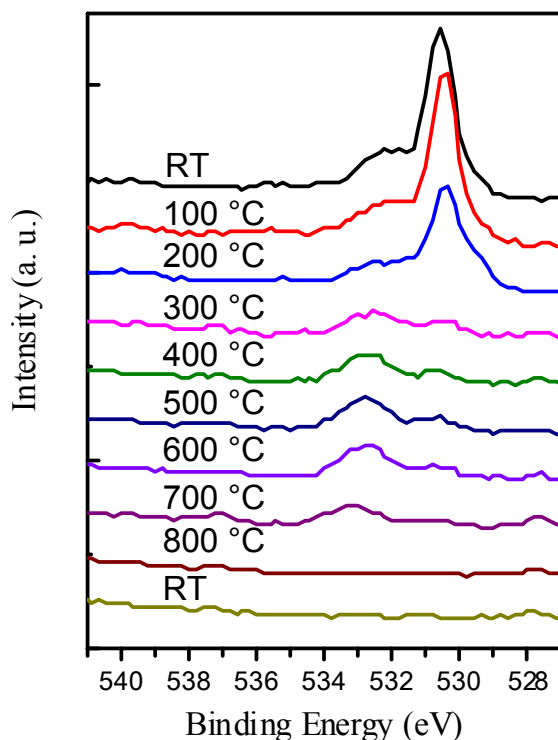


Figure S6. O1s spectra obtained during *in situ* heating for the Cu foil after annealed in Ar for 65 min. The temperature was elevated from RT (top spectrum) to 800 °C and then naturally cooled down to RT (bottom).

7. Verification of the Cu₂O Thickness Formed by Ar Annealing

The samples were prepared with fixed H₂/Ar annealing time (15 min) and different Ar annealing time (0, 20, and 100 min), and were then cooled down under Ar ambient without the growth process. The samples after the CVD process were transferred to the XPS chamber within 15.5–18 min. XPS depth profiling with more than 4 points in each sample were obtained.

Figure S7a shows the dependence of atomic ratio of oxygen (O/Cu + O) on depth from surface of Cu foils with different Ar annealing time. Figure S7b shows the thickness of Cu oxide formed by different Ar annealing time. The thicknesses of Cu oxide in Figure S7b were defined by the depth where the oxygen signal becomes zero in Figure S7a. The average thicknesses of Cu oxide after the Ar annealing for 0, 20, and 100 min are 2.0 ± 0.3 , 3.0 ± 0.3 , and 5.5 ± 1.0 nm, respectively (Figure S7b). The variation in the oxide thickness would be due to small time difference of the transferring sample from XPS to CVD chamber, difference of sputtering yield for each sample, sample positions, and different oxidation rates across different Cu orientation. Since the standard errors are sufficiently small, this result indicates the longer Ar annealing resulting in thicker Cu oxide layer. The statistical analysis also guarantees the reproducibility of these experiments.

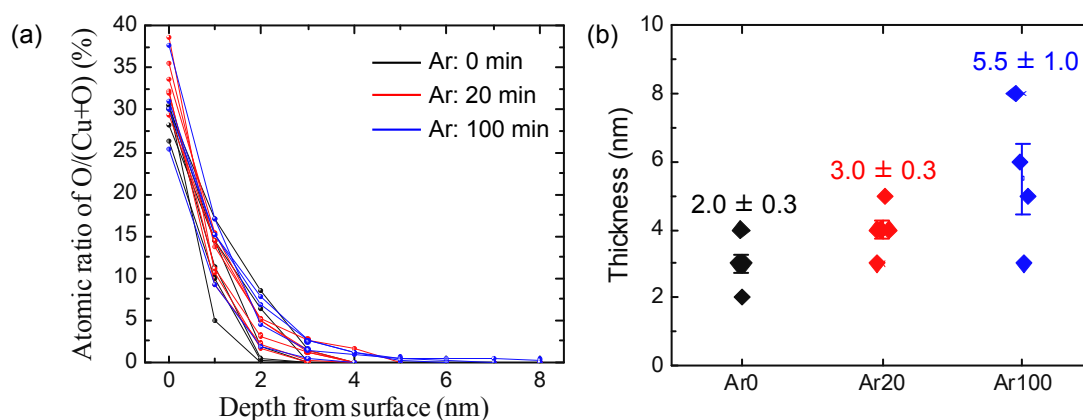


Figure S7. (a) Dependence of atomic ratio of oxygen on depth from surface of Cu foils with different Ar annealing time; (b) Dependence of the thickness of Cu oxide on Ar annealing time. Ar0, Ar20, and Ar100 as the name of samples are corresponding to the samples treated by Ar annealing for 0, 20, and 100 min, respectively. The numerical numbers above each plot indicate averages and standard errors of the thickness of Cu oxide. Transfer process from the CVD to the XPS chamber took roughly 16.5, 15.5, and 18.0 min for Cu foils with Ar annealing for 0, 20, and 100 min, respectively.

8. Electron Backscatter Diffraction Measurement of Annealed Cu Foils

Electron backscatter diffraction (EBSD) patterns were obtained by field-emission scanning electron microscope (SU6600, Hitachi, Japan). The Cu for the EBSD was heated in Ar following by H₂/Ar annealing for 2.5 h at 1035 °C.

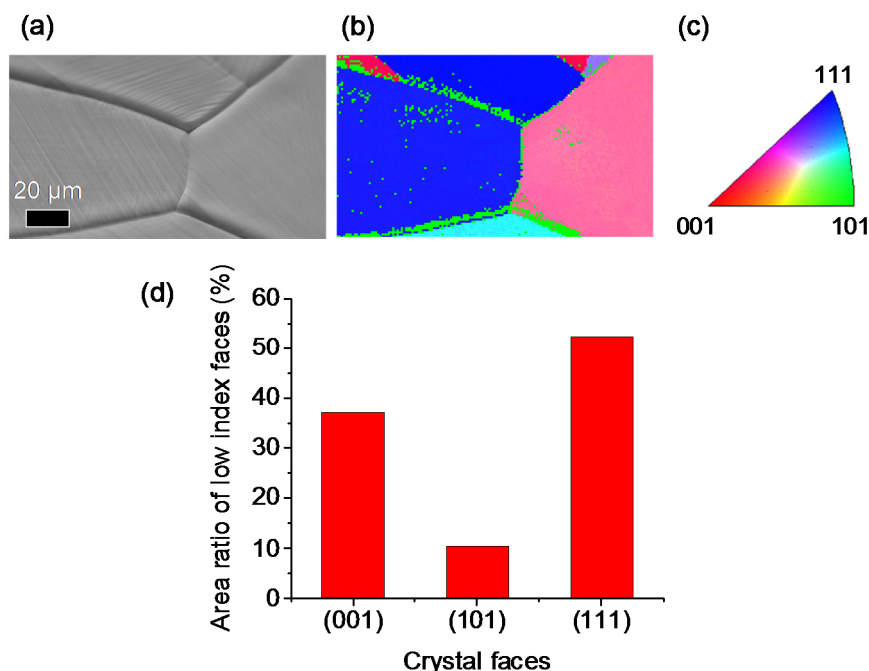


Figure S8. Electron backscatter diffraction (EBSD) analysis of a Cu foil which was heated in Ar following by H₂/Ar annealing for 2.5 h. (a) Scanning electron microscope image of Cu surface; (b) Corresponding EBSD orientation color map. The color represents the fcc crystalline orientation shown in (c); (d) Area ratio of low index faces for the annealed Cu foil.

9. Low Energy Electron Diffraction (LEED) Pattern of a Large-Sized Hexagonal Graphene Domain with the Size of ~1 mm

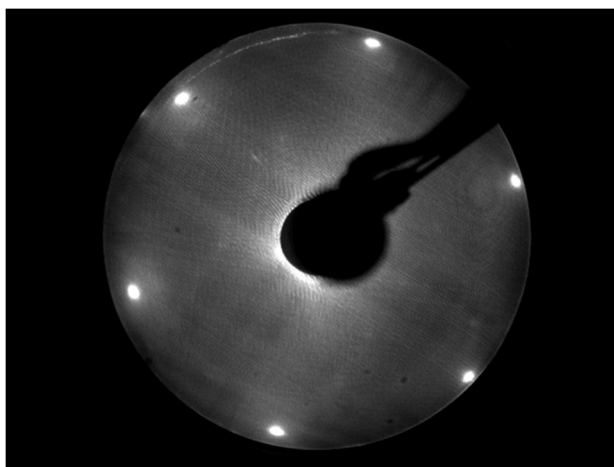


Figure S9. LEED pattern from a large-sized hexagonal graphene domain on Cu. The size of the graphene domain is ~1 mm. The spot size of the electron beam is approximately 1 mm, and the incident electron energy is 70 eV. The six-folded symmetrical LEED pattern was observed and the pattern was not changed by moving the beam position, indicating that the hexagonal graphene domain is single crystal.

Reference

- 1 Magnuson, G.D.; Carlston, C.E. Sputtering yields of single crystals bombarded by 1- to 10-keV Ar⁺ ions. *J. Appl. Phys.* **1963**, *34*, doi:10.1063/1.1729175.
2. Platzman, I.; Brener, R.; Haick, H.; Tannenbaum, R. Oxidation of Polycrystalline copper thin films at ambient conditions. *J. Phys. Chem. C* **2008**, *112*, 1101–1108.